Energy-Efficient Homing Control of Underactuated Marine Vehicles under Faulty Actuator Conditions

Dictino Chaos García[0000−0003−0132−785X] and
Cristina Cerrada Collado[0009−0003−4452−405X]

Abstract Each chapter should be preceded by an abstract (no more than 200 words) that summarizes the content. The abstract will appear *online* at www.SpringerLink.com and be available with unrestricted access. This allows unregistered users to read the abstract as a teaser for the complete chapter.

Please use the 'starred' version of the `abstract` command for typesetting the text of the online abstracts (cf. source file of this chapter template `abstract`) and include them with the source files of your manuscript. Use the plain `abstract` command if the abstract is also to appear in the printed version of the book.

1 Introduction

The marine environment is challenging and can sometimes cause damage to the actuators of marine vehicles. The situation in which vehicles are under faulty actuator conditions is undesirable, especially during a mission. Once a failure occurs in a vehicle, it is important to maintain control of the vehicle. For this reason, fault-tolerant control is a topic of interest nowadays.

Depending on the number of actuators on the vehicle, different approaches to fault-tolerant control can be found in the literature. Many vehicles are over-actuated, so they have plenty of actuators to control the vehicle in all 6 degrees of freedom (DOF). When an actuator fails, the common fault-tolerant control strategy is to compensate with the remaining actuators. For example, in [13] and [16] the existence of redundant actuators for an AUV (Autonomous Underwater Vehicle) is exploited to overcome failures during

Dictino Chaos García
Department of Computer Science and Automatic Control, National Distance Education University (UNED), C/ Juan del Rosal 16, 28040, Madrid, Spain, e-mail: dchaos@dia.uned.es

Cristina Cerrada Collado
Department of Computer Science and Automatic Control, National Distance Education University (UNED), C/ Juan del Rosal 16, 28040, Madrid, Spain, e-mail: criscerrada@dia.uned.es

operation by actuator force allocation of the remaining actuators. In [14] the authors address the dynamic modelling of an AUV's propulsion system and fault-tolerant control by reallocating actuator control forces. In [6] a dynamic surface fault-tolerant control system for ROV (Remotely Operated Vehicle) is presented for use in trajectory tracking operations. The fully-actuated vehicle uses a fault-tolerant actuator allocation policy to distribute the moment and forces among the remaining actuators, achieving good performance in tracking operations.

Other studies examine situations in which actuator failure reduces the vehicle's degrees of freedom. For example, in [5] geometric control theory is used to design trajectories to recover an AUV after an actuator failure, which reduces the available DOF and makes the vehicle underactuated. The AUV is modelled as a forced, affine connection control system. Control is carried out using integral curves of rank one and kinematic reductions. In [3] the authors propose an online learning-based method for finding control policies to deal with actuator failures. This method is applied to a fully-actuated vehicle that may become underactuated if one of the actuators fails. To this end, the fault-tolerant policy is represented by a linear function approximator, whose parameters are learned depending on the AUV model and the mission. The AUV model is learnt on board and adapted in the event of a failure. In [21] a fault-tolerant control for underactuated vehicles has been developed using a composite neural learning fault-tolerant control for path following that considers event-triggered input. The actuator faults considered are partial loss of effectiveness and bias fault. The reader is referred to [4] for a deeper review on fault-tolerant control systems and approaches.

In the event of a critical failure, it is desirable to drive the vehicle home, i.e. to a safe area where it can be recovered. In contrast to the above mentioned works, the extreme situation of controlling an underactuated AUV that experiences a critical failure is considered in [9]. This failure drastically reduces the DOF of the vehicle and leaves it with only one actuator available. Control is performed on the horizontal plane and allows the vehicle to be driven in a desired direction by switching between two control actions.

Since many marine vehicles should work autonomously over extended periods of time, energy consumption is also a critical factor to be considered. For this reason, the focus of a variety of works is on optimising energy consumption. For example, in [19] energy consumption is directly affected by the rudder angle control. In order to adaptively adjust trajectory tracking performance or energy consumption, a weight coefficient is introduced in the optimisation. In [20], the authors address the issue of reducing energy consumption by using Model Predictive Control (MPC) based on a state-space model of an over-actuated AUV for trajectory tracking control. To this end, a quadratic energy consumption term is added into the cost function. In [18] a Liner-Quadratic Regulator (LQR) controller is proposed to stabilise the pitch angle and heave motion and reduce energy consumption, with the parameters optimised using Genetic Algorithms (GA). In [12] a detailed energy consumption model for an underactuated AUV is developed that explicitly incorporates its propulsion system (DC motor and actuators with propellers) and hydrodynamic drag. The model is employed to estimate the energy expended when executing a trajectory, so it is a key ingredient in the computation of an energy-optimal strategy for the vehicle to perform a given task.

The possibility of actuator failure has not been considered in previous works. Nevertheless, in [15], the optimisation of a fault-tolerant control allocation technique in conjunction with energy consumption for an overactuated AUV is investigated. The square of actuator forces is used to minimise the energy consumption of the actuators. In [10] a complete fault-tolerant system is presented for a fully-actuated AUV. This system uses an actuator allocation algorithm to compensate for a faulty actuator. The algorithm is optimised to take into account actuator energy consumption. Finally, in [8] the scenario where a critical failure leaves an underactuated AUV with only one actuator available is studied again. In the event of this critical failure, an optimal control law to drive the vehicle to a recovery point is proposed. This control law allows for a trade-off between energy consumption and reaching the recovery point faster.

It is against this background of ideas that in this chapter, taking as a basis [9], the design of various control strategies for driving an underactuated AUV to a recovery point (so-called homing manoeuvre) using only one available actuator is presented. The aim is to provide a practical approach that helps readers intuitively understand the path taken to obtain the control solution published in [9]. Then, following the content published in [7], different options for improving this control are explored. To this end, an optimisation problem is posed in order to find the optimal control. The energy-efficient control strategy presented in [8] is also analysed. In addition, online material has been prepared so that readers can interact with the various controls presented.

The main contributions of the chapter are:

- A practical approach to explaining control strategies.
- Additional material to interact with the various controls presented.

The rest of the chapter is organised as follows. Section 2 introduces the model of the underactuated vehicle used. Section 3 analyses and discusses the design of the discrete control in [9]. Section 4 formulates the optimisation problem to find the optimal control and explores different solutions. Section 5 studies the energy-efficient control. Finally, the main conclusions are summarised in Section 6.

2 Vehicle model

The marine vehicle considered for the design of fault-tolerant control is the MEDUSA Class AUV (see Fig. 1). The vehicle is composed of two connected torpedo shaped acrylic bodies, placed one above the other, and attached to an aluminium frame. It has two stern horizontal actuators and two vertical actuators. This configuration allows control of surge and yaw rate with the horizontal actuators, and depth and roll with the vertical actuators. Furthermore, roll and pitch are negligible considering the stability of these movements provided by the design features. The vehicle can therefore manoeuvre in 3+1 DOF, which means 3 DOF in XY plane and 1 DOF in Z-axis. This makes it an underactuated AUV. The vehicle is designed with positive buoyancy, meaning that the upper tube remains on the surface and the lower tube remains underwater unless the vertical actuators are commanded for diving. The reader is referred to [1] for a deeper review of the features of the MEDUSA-class vehicles.

Fig. 1 MEDUSA Class AUV [9].

In the event of a failure, the vehicle emerges to the surface due to its positive buoyancy. For this reason, the control of the vehicle is studied in the horizontal plane, i.e. in 2D, once the vehicle is at the sea surface.

The model for underwater vehicles described in [11] is divided into two parts: kinematics and kinetics. The kinematics focuses on geometrical aspects of the vehicle motion as the rotation of the velocities and the kinetics analyses the forces causing the motion.

The vehicle model is described using two reference frames that follow the standard convention SNAME [17], the body-frame and the inertial one (see Fig. 2). The origin of the AUV body-frame is located at its centre of mass. The speeds of the vehicle referred to the body-frame are $\boldsymbol{\nu} = [u\ v\ r]^T$, where u is surge speed, v is sway speed, and r is

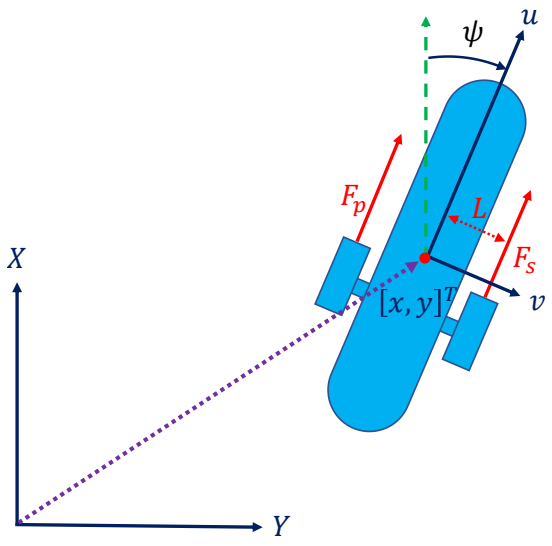

Fig. 2 Graphical representation of the forces applied to the AUV by the actuators, AUV speeds in the body-frame and AUV position in the inertial coordinate frame [9].

yaw rate. The velocity in the inertial frame is $\mathbf{V} = [\dot{x}, \dot{y}, \dot{\psi}]^T$, where $\dot{x}$ is the speed along X-axis, which points north, and $\dot{y}$ is the speed along the Y-axis, which points to the east, ψ is the angle that the vehicle orientation forms with the X-axis and its derivative $\dot{\psi} = r$ is the yaw rate. Then, in the absence of ocean currents, the kinematic model of the vehicle yields

$$\dot{x} = u \cdot \cos(\psi) - v \cdot \sin(\psi) \tag{1}$$

$$\dot{y} = u \cdot \sin(\psi) + v \cdot \cos(\psi) \tag{2}$$

$$\dot{\psi} = r \tag{3}$$

When the vehicle is at the surface, it is controlled by the horizontal actuators, whose inputs a_s and a_p are the angular velocity references for the starboard and portside actuator propellers, respectively. These inputs are given in terms of standard dimensionless reference commands for the internal controller of the propellers in the non-dimensional range $[-100, 100]$. To obtain the true propeller rotations, a conversion from the non-dimensional commands is needed, e.g. the portside propeller rotational velocity (in rad/s) w_p is computed through the portside propeller rotational velocity n_p (in rps) that depends on a_p and on the maximum propeller rotational velocity n_{max} (in rps), see equations (4 - 5). Similarly, the starboard propeller rotational velocity could be calculated.

$$n_p = n_{max} \cdot a_p/100, \tag{4}$$

$$w_p = 2 \cdot \pi \cdot n_p. \tag{5}$$

Each propeller produces a thrust whose magnitude is proportional to the square of its own angular velocity and its sign is the same as the angular velocity. Thus, the thrust is positive (pushes forward) if control action is positive and negative (pushes backward) if the control action is negative. In accordance, the forces produced in response to the command references are described by

$$F_s(a_s) = K \cdot |a_s| \cdot a_s, \tag{6}$$

$$F_p(a_p) = K \cdot |a_p| \cdot a_p, \tag{7}$$

where K is the proportional constant that relates the command references to the force produced. The total force applied to the vehicle results from the summation of the forces of both actuators $F = F_p(a_p) + F_s(a_s)$, which also produces the torque $\tau = L \cdot (F_p(a_p) - F_s(a_s))$, where L is the distance of each of the actuators to the symmetry axis of the vehicle, see Fig. 2.

As mentioned above, the problem under study is the one in which one of the actuators has been damaged and cannot be operated. Without loss of generality, the starboard actuator has been selected as the faulty one. In this case, only the portside thuster is active and generates the total force and moment $F = F_p(a_p)$ and $\tau = L \cdot F_p(a_p)$, respectively, allowing only for partial control of the surge speed and yaw rate. According to [11], [2] and taking into account the particularities of the case study, the dynamic model is rewritten as

$$m_u \cdot \dot{u} - m_v \cdot v \cdot r + D_u(u) \cdot u = F = F_p(a_p), \tag{8}$$

$$m_v \cdot \dot{v} + m_u \cdot u \cdot r + D_v(v) \cdot v = 0, \tag{9}$$

$$m_r \cdot \dot{r} - m_{uv} \cdot u \cdot v + D_r(r) \cdot r = \tau = L \cdot F_p(a_p), \tag{10}$$

where m_u, m_v and m_r are the mass and inertia constants that take into account so-called added masses due to water, and $m_{uv} = m_u - m_v$. Due to the rotation of the body-frame, the Coriolis terms appear as $v \cdot r$, $u \cdot r$, and $u \cdot v$. Finally, the drag terms $D_u(u)$, $D_v(v)$, and $D_r(r)$ are produced by the dissipating forces of the water, defined as

$$D_u(u) = -X_u - X_{|u|} \cdot |u|, \tag{11}$$

$$D_v(v) = -Y_v - Y_{|v|} \cdot |v|, \tag{12}$$

$$D_r(r) = -N_r - N_{|r|} \cdot |r|, \tag{13}$$

where $X_u, X_{|u|}, Y_v, Y_{|v|}, N_r, N_{|r|}$ are the hydrodynamic coefficients, which are negative and $D_u(u)$, $D_v(v)$ and $D_r(r)$ are positive.

Finally, the model parameters used are shown in Table 1.

Table 1 MEDUSA-class vehicle model parameters.

Parameter	Value
m_u	$37\ kg$
m_v	$47\ kg$
m_r	$4.64\ kg \cdot m^2$
X_u	$-0.2\ kg \cdot s^{-1}$
Y_v	$-55.1\ kg \cdot s^{-1}$
N_r	$-4.14\ kg \cdot m^2 \cdot s^{-1}$
$X_{\|u\|u}$	$-25\ kg \cdot m^{-1}$
$Y_{\|v\|v}$	$-101.3\ kg \cdot m^{-1}$
$N_{\|r\|r}$	$-6.23\ kg \cdot m^2$
K	$3.6 \cdot 10^{-3}\ N$
L	$0.25\ m$

3 Discrete Control

The aim is to design a control action over a_p so that the system (1)-(10) converges to a neighbourhood of the origin from any initial condition, i.e., the AUV can be driven with the use of a single actuator to a desired (recovery) area.

It is important to notice that, as the single control action a_p is used and it impacts directly on both the surge speed u and the yaw rate r, it is not possible to make the vehicle follow a straight path with a certain desired reference surge speed and orientation, as it would be expected if both control actions a_s and a_p could be applied.

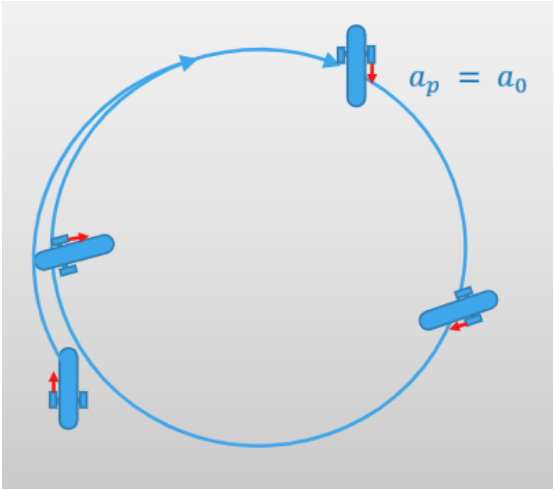

Fig. 3 Result of applying constant control action $a_p = a_0$ to the AUV.

Proposal 1

What would happen if one tried to control the AUV by applying a constant force?

As can be seen in Fig. 3, if a constant control action is applied to the available actuator, for example $a_p = a_0$, the vehicle will remain turning in circles, and the average advance velocity is zero.

In order to obtain an non-zero average advance velocity, the symmetry of the circular trajectory must be broken, so a constant input control action is not suitable.

Proposal 2

What would happen if one tried to control the AUV by applying more force when the vehicle points to the East and less force when it points to the West?

The control law that allows two control actions to be applied, switching depending on the orientation of the vehicle, is $a_p = a_0 + \Delta a \cdot sign(\sin(\psi))$.

This control law works as follows: Consider that the vehicle turns clockwise ($r > 0$) describing an approximately circular trajectory (for Δa small) and pointing to the interior of the circular path because $u > 0$ and $v < 0$. Therefore, the velocity vector of the vehicle, which is tangent to the trajectory, points to port. When $\psi = 2n\pi$ the vehicle points exactly to the North, which is the frontier at which the vehicle changes its orientation from West to East (point A of Fig. 4), and a_p

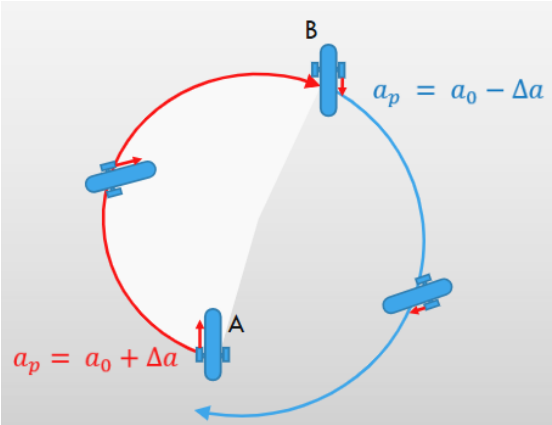

Fig. 4 Result of applying the control law $a_p = a_0 + \Delta a \cdot sign(\sin(\psi))$ to the AUV. When the vehicle points to the East, the control action is $a_p = a_0 + \Delta a$ (more force) and it is represented in red. When the vehicle points to the West, the control action is $a_p = a_0 - \Delta a$ (less force) and it is represented in blue.

switches from $a_p = a_0 - \Delta a$ to $a_p = a_0 + \Delta a$, following the red path of Fig. 4. Once ψ reaches $(2n + 1)\pi$, the vehicle points exactly to the South (point B of Fig. 4) and the control law switches again to $a_p = a_0 - \Delta a$, describing the blue path. Since the control action is different in both parts of the path (red and blue) the trajectory does not close, i.e. it is not a circumference. This pattern is repeated periodically producing an average movement of the vehicle on a certain course.

Although the choice of when to apply more or less force is a little arbitrary, the vehicle moves and no longer remains turning in circles.

The drawback of **Proposal 2** is that it is impossible to predict the direction in which the vehicle is moving. The direction of the average movement depends on many things in a complex way, but it is easy to measure (see Fig. 5). However, it is needed that the vehicle moves along a desired direction.

Proposal 3

What would happen if one tried to modify **Proposal 2** to move the vehicle along a predefined desired direction ψ_r?

The direction in which the vehicle is moving can be corrected by adding an offset to the orientation. Thus, the control law yields: $a_p = a_0 + \Delta a \cdot sign(\sin(\psi + \Delta\psi - \psi_r))$.

This control law switches when $\psi = \psi_r - \Delta\psi + 2n\pi$ and $\psi = \psi_r - \Delta\psi + (2n+1)\pi$, as shown in Fig. 6, and the vehicle moves in direction ψ_r instead of moving in direction $\Delta\psi$ with respect to the X-axis. Doing this way, the trajectory obtained

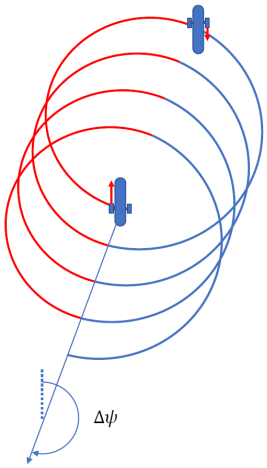

Fig. 5 The direction of the average velocity when the control law of **Proposal 2** is applied, $\Delta\psi$.

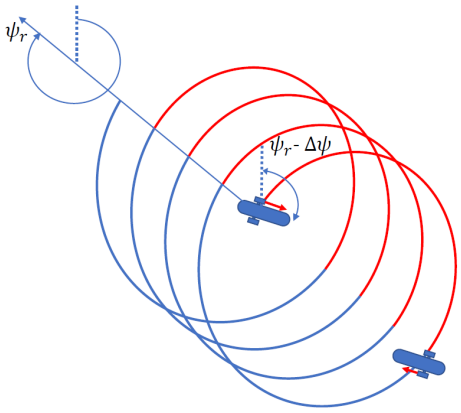

Fig. 6 Result of applying the control law $a_p = a_0 + \Delta a \cdot sign(\sin(\psi + \Delta\psi - \psi_r))$ to the AUV.

is rotated an angle $\psi_r - \Delta\psi$ with respect to the trajectory obtained in **Proposal 2**, and the final average velocity points towards $\Delta\psi + \psi_r - \Delta\psi = \psi_r$.

Now that a control law has been designed that allows the AUV to be driven in a desired direction using only one actuator, the aim is to prove mathematically that it works. The control law is non linear, non standard and discontinuous since it switches between two control actions. For that reasons, showing that it works is a laborious task. The complete demonstration can be found in [9], but the main ideas of the proof are presented below.

It is needed to prove that a limit cycle (sustained oscillation) exist for the velocities, then:

1. If the control action is constant, the vehicle tends to stable body-frame velocities ($a_p = a_0 \pm \Delta a$).
2. The control switches when it reaches a switching surface ($sin(...) = 0$).
3. It switches infinitely many times. So, look what happens at the switching points.
4. Look what happens to close trajectories.

   a. If they approach each other, then it is contractive, it exist an attractive fixed point.
   b. It is needed to show that this fixed point has an average velocity $\neq 0$

Once the control has been demonstrated to work, the final step is to select the desired recovery point (set point) and determine the direction towards it.

Final control

Computing the desired direction ψ_r using the position of the vehicle $[x, y]^T$ and the position of the recovery point $[x_r, y_r]^T$, the final control is

$$\psi_r(x, y) = atan2(y_r - y, x_r - x) \tag{14}$$

$$a_p = a_0 + \Delta a \cdot (\sin(\psi + \Delta\psi - \psi_r(x, y))) \tag{15}$$

4 Optimal Control

An optimisation problem that finds the control action to minimise the integral square error of the vehicle's trajectory with respect to the desired recovery point is proposed. For this purpose, two different control strategies are considered. The first strategy studies a control signal sampled in time and uses the control actions at each sampling instant as the parameter to be optimised. The second strategy analyses a control law as a function of the orientation of the AUV with respect to the target point and represents this function by means of a Fourier series.

5 Energy-Efficient Control

6 Conclusions

References

1. Abreu, P.C., Botelho, J., Góis, P., Pascoal, A., Ribeiro, J., Ribeiro, M., Rufino, M., Sebastião, L., Silva, H.: The MEDUSA class of autonomous marine vehicles and their role in EU projects. In: OCEANS 2016 - Shanghai, pp. 1–10 (2016). DOI 10.1109/OCEANSAP.2016.7485620
2. Aguiar, A., Pascoal, A.: Regulation of a nonholonomic autonomous underwater vehicle with parametric modeling uncertainty using Lyapunov functions. In: Decision and Control, 2001.

Proceedings of the 40th IEEE Conference on, vol. 5, pp. 4178 –4183 vol.5 (2001). DOI 10.1109/.2001.980841
3. Ahmadzadeh, S.R., Leonetti, M., Carrera, A., Carreras, M., Kormushev, P., Caldwell, D.G.: Online discovery of auv control policies to overcome thruster failures. In: 2014 IEEE International Conference on Robotics and Automation (ICRA), pp. 6522–6528 (2014)
4. Amin, A.A., Hasan, K.M.: A review of Fault Tolerant Control Systems: Advancements and applications. Measurement **143**, 58–68 (2019). DOI https://doi.org/10.1016/j.measurement.2019.04.083
5. Andonian, M., Cazzaro, D., Invernizzi, L., Chyba, M., Grammatico, S.: Geometric control for autonomous underwater vehicles: Overcoming a thruster failure. In: 49th IEEE Conference on Decision and Control (CDC), pp. 7051–7056 (2010)
6. Baldini, A., Ciabattoni, L., Felicetti, R., Ferracuti, F., Freddi, A., Monteriù, A.: Dynamic surface fault tolerant control for underwater remotely operated vehicles. ISA Transactions **78**, 10–20 (2018). DOI https://doi.org/10.1016/j.isatra.2018.02.021
7. Cerrada, C., Chaos, D., Moreno-Salinas, D., Aranda, J.: Optimal control law of an auv using a single thruster. Revista Iberoamericana de Automática e Informática industrial (2023). DOI 10.4995/riai.2023.19034
8. Cerrada, C., Chaos, D., Moreno-Salinas, D., Pascoal, A., Aranda, J.: An energy efficient fault-tolerant controller for homing of underactuated AUVs. Control Engineering Practice **146**, 105883 (2024). DOI 10.1016/j.conengprac.2024.105883. URL https://www.sciencedirect.com/science/article/pii/S0967066124000431
9. Chaos, D., Moreno-Salinas, D., Aranda, J.: Fault-Tolerant Control for AUVs Using a Single Thruster. IEEE Access **10**, 22123–22139 (2022). DOI 10.1109/ACCESS.2022.3152190. Conference Name: IEEE Access
10. De Carolis, V., Maurelli, F., Brown, K.E., Lane, D.M.: Energy-aware fault-mitigation architecture for underwater vehicles. Autonomous Robots **41**(5), 1083–1105 (2017). DOI 10.1007/s10514-016-9585-x. URL https://doi.org/10.1007/s10514-016-9585-x
11. Fossen, T.I.: Marine Control Systems: Guidance, Navigation and Control of Ships, Rigs and Underwater Vehicles. Marine Cybernetics AS, Trondheim (2002)
12. Häusler, A.J.: Mission Planning for Multiple Cooperative Robotic Vehicles. Ph.D. thesis, UNIVERSIDADE DE LISBOA INSTITUTO SUPERIOR TÉCNICO (2015)
13. Podder, T.K., Sarkar, N.: Fault-tolerant control of an autonomous underwater vehicle under thruster redundancy. Robotics and Autonomous Systems **34**(1), 39 – 52 (2001). DOI https://doi.org/10.1016/S0921-8890(00)00100-7
14. Rauber, J.G., Santos, C.H.F.d., Chiella, A.C.B., Motta, L.R.H.: A strategy for thruster fault-tolerant control applied to an AUV. In: 2012 17th International Conference on Methods Models in Automation Robotics (MMAR), pp. 184–189 (2012)
15. Saback, R., Cesar, D., Arnold, S., Lepikson, H., Santos, T., Albiez, J.: Fault-tolerant control allocation technique based on explicit optimization applied to an autonomous underwater vehicle. In: OCEANS 2016 MTS/IEEE Monterey, pp. 1–8 (2016). DOI 10.1109/OCEANS.2016.7761251
16. Sarkar, N., Podder, T.K., Antonelli, G.: Fault-accommodating thruster force allocation of an AUV considering thruster redundancy and saturation. IEEE Transactions on Robotics and Automation **18**(2), 223–233 (2002)
17. SNAME: Nomenclature for Treating the Motion of a Sumerged Body Through a Fluid. Tech. rep., The Society of naval Architects and Marine Engineers (1950). Series: Technical and research bulletin Nº 3-47
18. Wang, S., Jin, H., Meng, L., Li, G.: Optimize motion energy of AUV based on LQR control strategy. In: 2016 35th Chinese Control Conference (CCC), pp. 4615–4620 (2016). DOI 10.1109/ChiCC.2016.7554068. ISSN: 1934-1768
19. Xia, Y., Xu, K., Huang, Z., Wang, W., Xu, G., Li, Y.: Adaptive energy-efficient tracking control of a X rudder AUV with actuator dynamics and rolling restriction. Applied Ocean Research **118**, 102994 (2022). DOI 10.1016/j.apor.2021.102994
20. Yao, F., Yang, C., Zhang, M., Wang, Y.: Optimization of the Energy Consumption of Depth Tracking Control Based on Model Predictive Control for Autonomous Underwater Vehicles. Sensors **19**(1), 162 (2019). DOI 10.3390/s19010162. Number: 1 Publisher: Multidisciplinary Digital Publishing Institute

21. Zhang, G., Chu, S., Jin, X., Zhang, W.: Composite neural learning fault-tolerant control for underactuated vehicles with event-triggered input. IEEE Transactions on Cybernetics **51**(5), 2327–2338 (2021). DOI 10.1109/TCYB.2020.3005800